The International Journal of Cardiovascular Imaging (2024) 40:801–809
https://doi.org/10.1007/s10554-024-03049-3

ORIGINAL PAPER

Assessment of myocardial strain patterns in patients with left bundle branch block using cardiac magnetic resonance

Marina Raquel Santos[1,2] · Mariana Santos Silva[2,3] · Sara Lopes Guerreiro[2] · Daniel Alberto Gomes[2] · Bruno Miguel Rocha[2] · Gonçalo Lopes Cunha[2] · Pedro Nuno Freitas[2] · João Maria Abecasis[2] · Ana Coutinho Santos[2] · Carla Cristina Saraiva[2] · Miguel Mendes[2] · António Miguel Ferreira[2]

Received: 7 September 2023 / Accepted: 5 January 2024 / Published online: 20 February 2024

Abstract

Recently, a classification with four types of septal longitudinal strain patterns was described using echocardiography, suggesting a pathophysiological continuum of left bundle branch block (LBBB)-induced left ventricle (LV) remodeling. The aim of this study was to assess the feasibility of classifying these strain patterns using cardiovascular magnetic resonance (CMR), and to evaluate their association with LV remodeling and myocardial scar. Single center registry included LBBB patients with septal flash (SF) referred to CMR to assess the cause of LV systolic dysfunction. Semi-automated feature-tracking cardiac resonance (FT-CMR) was used to quantify myocardial strain and detect the four strain patterns. A total of 115 patients were studied (age 66 ± 11 years, 57% men, 28% with ischemic heart disease). In longitudinal strain analysis, 23 patients (20%) were classified in stage LBBB-1, 37 (32.1%) in LBBB-2, 25 (21.7%) in LBBB-3, and 30 (26%) in LBBB-4. Patients at higher stages had more prominent septal flash, higher LV volumes, lower LV ejection fraction, and lower absolute strain values ($p < 0.05$ for all). Late gadolinium enhancement (LGE) was found in 55% of the patients (n = 63). No differences were found between the strain patterns regarding the presence, distribution or location of LGE. Among patients with LBBB, there was a good association between strain patterns assessed by FT-CMR analysis and the degree of LV remodeling and LV dysfunction. This association seems to be independent from the presence and distribution of LGE.

Keywords LBBB · Septal flash · Strain patterns · FT-CMR · LV remodeling

Abbreviations

CMR	Cardiovascular magnetic resonance
CRT	Cardiac resynchronization therapy
FT-CMR	Feature-tracking cardiac resonance
GCS	Global circumferential strain
GLS	Global longitudinal strain
GRS	Global radial strain
LBBB	Left bundle branch block
LGE	Late gadolinium enhancement
LV	Left ventricle
LVEF	Left ventricle ejection fraction
SF	Septal flash
STE	Speckle tracking echocardiographic

✉ Marina Raquel Santos
m.raquel.santo1992@gmail.com

[1] Hospital Dr. Nélio Mendonça, Funchal, Portugal

[2] CHLO - Hospital de Santa Cruz, Lisbon, Portugal

[3] Centro Hospitalar Barreiro/Montijo, Setúbal, Portugal

Introduction

Over the years, our understanding of left bundle branch block (LBBB) has evolved from a simple electrocardiographic finding to a clinical entity that may cause left ventricular remodeling and dysfunction in the absence of myocardial disease [1]. LBBB has been known to result in electromechanical ventricular dyssynchrony, and adversely affect prognosis by triggering structural remodeling, left ventricular (LV) dilatation, dysfunction, and heart failure (HF) [2]. The relationship between LBBB and LV dysfunction is complex and poorly understood, and identifying LBBB-induced adverse remodeling in individual patients is challenging [3]. Septal flash (SF) [4] and speckle tracking-based strain echocardiography [5] have emerged as useful tools in a broad range of settings. Among other uses, these tools may help explain the wide spectrum of effects that LBBB may have on the left ventricle, ranging from no discernable consequences to severe dilatation and systolic dysfunction. Recently, a speckle tracking echocardiographic

(STE) classification of LBBB-induced septal longitudinal strain patterns was proposed. This four-stage classification suggests a pathophysiological continuum of LBBB-induced LV remodeling [6].

Cardiovascular magnetic resonance (CMR) is considered the reference standard for the evaluation of biventricular morphology and function. Using late gadolinium enhancement (LGE), CMR also has the unique ability to identify replacement myocardial fibrosis, a common finding in patients with HF, and an important prognostic marker [7]. Feature tracking is also possible using CMR, but data regarding its applicability and clinical usefulness are still scarce [7–10].

The aim of this study was to assess the feasibility of using feature-tracking CMR (FT-CMR) to replicate the classification of LBBB-induced septal longitudinal strain patterns, and to evaluate their association with LV remodeling and LGE.

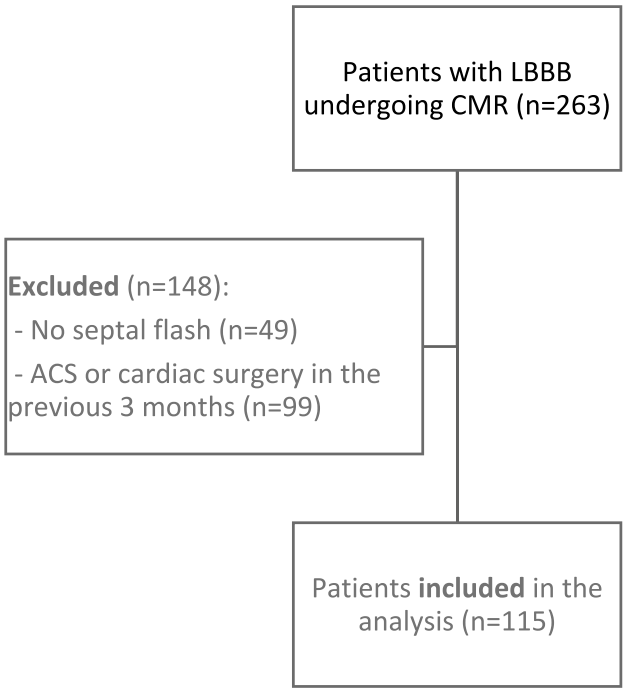

Fig. 1 Flow-chart of the study cohort. *LBBB* Left bundle branch block; *CMR* Cardiac magnetic resonance; *ACS* Acute coronary syndrome.

Methods

Study population

This was a single-center, retrospective, observational study that enrolled all patients with LBBB undergoing cardiac (CMR) in our center as part of the etiological evaluation of LV dysfunction (Fig. 1). Patients from November 2015 to November 2021 were included in the analyses. Individual consent was waived for using clinical data.

LBBB was defined according to Strauss criteria as strict LBBB, non-strict LBBB or nonspecific LV conduction delay [11, 12]. Strict LBBB was characterized by the presence of QS or rS in V1, QRS duration ≥ 140 ms in men or ≥ 130 ms in women and mid-QRS notching/slurring in at least two of the leads I, aVL, V1, V2, V5 or V6. In non-strict LBBB QS or rS in V1 and QRS duration ≥ 120 ms (not meeting the strict LBBB criteria) should be present. Non-LBBB LV conduction delay was defined by the presence of QS or rS in V1 and QRS duration 110–119 ms.

We excluded patients without septal flash (n = 49). Those with acute coronary syndrome or cardiac surgery (n = 99) during the previous 3 months were also excluded.

Relevant demographic and clinical data were retrospectively collected from the patient chart and electronic medical records. Ischemic heart disease was defined by subendocardial or transmural scar in LGE consistent with a coronary artery distribution territory.

Cardiac magnetic resonance imaging

All subjects were imaged using a 1.5 T scanner (Siemens Avanto®, Siemens Healthineers, Erlangen, Germany), using a standard CMR protocol [13], which included steady-state free precession cine imaging in standard cardiac views for strain analysis.

Ventricular volumes measurements were performed by experienced cardiologists and radiologists using dedicated software (Circle Cardiovascular Imaging 5.6.4®, Calgary, Canada).

The presence of septal flash, defined as a fast leftward motion of the septum during isovolumetric contraction [4] was visually assessed using ordinary cine sequences and scored as mild, moderate or prominent. The presence or absence of LGE and its location or distribution pattern were assessed qualitatively by using short and long-axis views. LGE distribution pattern was defined as subendocardial and as mid-wall/epicardial, and three different locations were considered (septal, lateral, and both) (Fig. 2). In 6 of the 115 patients LGE was not performed due to contraindications or refusal to receive gadolinium-based contrast agents.

Strain analysis using CMR

A semi-automated feature tracking (FT) technology (Circle CVI42®) was applied to the routinely acquired cine CMR images. After manually defining endocardial and epicardial borders in end-diastolic phase (excluding papillary muscles and trabeculae) the software performs automatic border tracking, estimating global longitudinal strain from

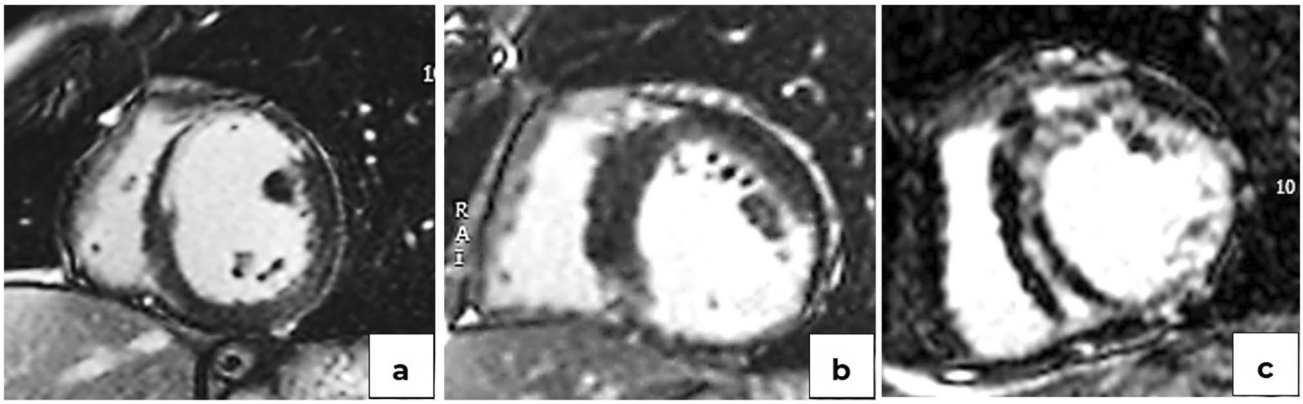

Fig. 2 Example of LGE in CMR short-axis views in three different patients: **a** Subendocardial LGE (ischemic scar) with septum involvement. **b** Subendocardial LGE in inferior and lateral wall. **c** Non-ischemic cardiomyopathy with midwall pattern of the septum and lateral wall- septal/lateral location

three long-axis SSFP cine images, and circumferential and radial strains from the short-axis cine images [7] (Fig. 3). The propagated myocardial tissue across the cardiac cycle was verified by the operator to ensure the accuracy of the propagation. Only good quality strain data were included, therefore all patients had proper image quality.

2D and 3D global radial strain (GRS), global circumferential strain (GCS) and global longitudinal strain (GLS) were derived. Using radial strain curves, lateral to septal wall peak strain delay was calculated as the difference in time to peak strain between the mid-septum and the opposing wall. Longitudinal strain curves of the mid-septum were analyzed to identify the LBBB pattern, according to the recent classification (LBBB-1 through LBBB-4) [6]. In LBBB-1, an early sigmoidal deflection was discerned, followed by late peak strain. In stage LBBB-2, an early small peak is followed by a larger dominant peak during ejection. The opposite occurs in stage LBBB-3, where a dominant early peak is followed by a smaller late peak [14]. In LBBB-4, an early peak strain of the septum is followed by stretching during further systole without ejection septal shortening [15]. We used the same reasoning to identify radial strain patterns.

All the measurements were analyzed by three different observers.

Statistical analysis

Continuous variables are expressed as mean ± SD or median ± interquartile range (IQR) with normal and non-normal distribution, respectively. Shapiro–Wilk test was used to test normality of the variables. The Student's t test or Mann–Whitney U test were used to compare two groups for parametric and non-parametric data, respectively. For paired data, paired Student's t-test and Wilcoxon signed rank test were used. Analysis of variance and Kruskal–Wallis testing were performed for comparison among multiple groups. Categorical variables are presented as count (percentage) and difference between groups were analyzed by chi-square tests or Fisher's exact test. A two-sided p-value < 0.05 was considered statistically significant. The statistical analysis

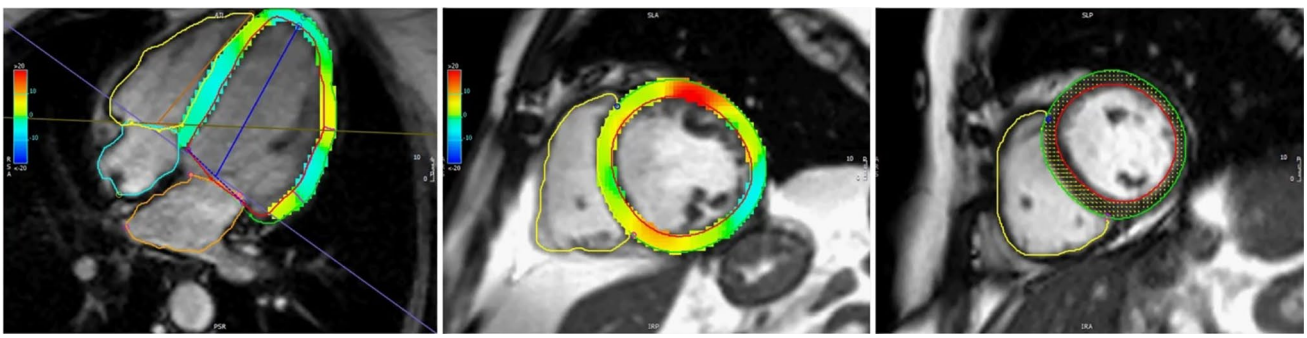

Fig. 3 Example of colored 2D strain analysis (apical four chamber view and short axis view) with CMR feature tracking software (Circle CVI42®). On the right column, the endocardial and epicardial borders of the left ventricle are marked by red and green contours, respectively, and the right ventricle by yellow

was performed with IBM SPSS Statistics 24.0 (IBM Corp, Armonk, NY, USA).

Results

Population baseline characteristics

A total of 115 patients with LBBB and SF were included. Table 1 summarizes the clinical, electrocardiographic and CMR characteristics of them. Briefly, the majority were classified as strict LBBB, and more than half had left ventricle ejection fraction (LVEF) under 35%. As per study design, all patients had SF, which was scored as mild in 36 (31%), moderate in 40 (35%) and prominent in 39 (34%).

Strain patterns

Four consistent mid-septal LBBB deformation patterns were obtained according to longitudinal and radial strain curves (Figs. 4 and 5). In longitudinal strain analyses LBBB-1 was observed in 23 (20%), LBBB-2 in 37 (32.1%), LBBB-3 in 25 (22%), and LBBB-4 in 30 (26%) patients. The clinical, electrocardiographic and CMR characteristics for each LBBB stage according to longitudinal septal strain pattern are shown in Table 1. A similar table according to radial septal strain pattern can be found in the supplementary material.

Staging LBBB-induced remodeling with strain imaging

Patients at higher LBBB stages (Table 1) had more prominent septal flash ($p < 0.001$), greater end-diastolic and end-systolic LV volumes ($p = 0.003$ and $p = 0.002$, respectively), lower LV ejection fraction ($p < 0.001$) and lower absolute global longitudinal ($p = 0.001$), circumferential ($p < 0.001$) and radial strain ($p = 0.002$) values compared with less advanced stages. Similar results were obtained with radial strain patterns (supplementary table, Fig. 6).

There was no difference between patterns in clinical characteristics, namely age, sex or ischemic etiology. Additionally, there was no difference between patterns and QRS duration ($p = 0.302$) or time delay between anterior IVS to posterior wall ($p = 0.297$).

Relation between LGE and strain patterns

LGE was found in 63 patients (54.8%), with a septal location in 34 (29.6%), lateral in 4 (3.5%) and both in 11 (9.6%) patients. Of these, 32 (27.8%) had an ischemic LGE pattern. Furthermore, no difference was found for LGE presence, distribution or location between the four strain patterns ($p = 0.846$ for longitudinal strain and $p = 0.464$ for radial strain) (Table 1 and supplementary).

Discussion

The major findings of our study can be summarized as follows: (1) CMR may be used to classify myocardial strain patterns in patients with LBBB; (2) the strain classification in four stages/patterns correlates with increasing degrees of LV remodeling, suggesting the existence of a pathophysiological continuum, and 3) the presence of LGE is similar across the different strain patterns, suggesting that myocardial scar is not a major determinant of these patterns.

LBBB is generally associated with a worse prognosis in comparison to normal intraventricular conduction or right bundle branch block [16] and might be the first manifestation of myocardial disease [17, 18]. LBBB-induced cardiomyopathy has received more attention since the introduction of cardiac resynchronization therapy (CRT), prompting the development of several techniques and criteria for the evaluation of potential candidates. In a recent classification Calle *et al* [6] described four longitudinal echocardiographic strain patterns (LBBB-1 to LBBB-4) in which patients at higher LBBB stages had greater LV volumes, lower LV ejection fraction and lower absolute GLS compared with patients in less advanced stages. Previous studies have also been described different echocardiographic longitudinal strain patterns in LBBB patients [15, 19, 20]. However, its applicability may be hindered by poor acoustic windows [21]. To the best of our knowledge, our study is one of the first aiming to replicate this classification using FT-CMR analysis in LBBB patients. CMR, less affected by image quality, is considered the gold standard for the evaluation of LV volumes and function [7], but there are little data on strain assessment in LBBB with this imaging modality [6, 8, 9, 22–25]. *Baritussio* et al. have shown that myocardial deformation assessed by CMR is impaired in LBBB patients when compared to healthy controls [26]. In addition, Land et al.have concluded that the presence of isolated LBBB seems to be associated with LV remodeling, diminished systolic function, mechanical dyssynchrony and tenting of the mitral valve apparatus [27].

Although STE plays a major role as first imaging modality [28] due to its low cost and widespread availability, our findings show that CMR can also be used to assess global strain values and patterns in patients with LBBB using standard cine images, which are routinely performed. In addition, we were able to reproduce not only longitudinal strain patterns but also to create the same concept for radial strain curves. In both radial and longitudinal strain patterns, our findings were consistent with a continuous progression of important features of cardiac remodeling and septal flash degree across

Table 1 Clinical, electrocardiographic and CMR characteristics of patients with LBBB-SF according to **Longitudinal** Septal Strain Pattern

	All Patients (n = 115)	Stage LBBB-1 (n = 23)	Stage LBBB-2 (n = 37)	Stage LBBB-3 (n = 25)	Stage LBBB-4 (n = 30)	P value	P value for trend
Clinical Characteristics							
Age (yrs)	66.0 ± 11.7	63.1 ± 11.9	66.0 ± 9.7	65.6 ± 11.5	68.8 ± 13.7	0.365	
Male	65 (56.5%)	10 (43.5%)	22 (59.5%)	15 (60.0%)	18 (60.0%)	0.574	
BMI (Kg/m^2)	26.1 (5.5)	25.1 (5.1)	26.7 (6.1)	25.1 (7.4)	26.9 (3.8)	0.772	0.960
Ischemic HF	32 (27.8%)	6 (26.1%)	10 (27.0%)	8 (32.0%)	8 (26.7%)	0.963	
QRS duration (ms)	150.0 (26.0)	150.0 (34.0)	148.0 (25.0)	150.0 (36.0)	150.0 (21.0)	0.302	0.080
LBBB according to Strauss criteria						0.460	
Strict LBBB	90 (78.3%)	15 (65.2%)	28 (75.7%)	22 (88%)	25 (83.3%)		
Non-strict LBBB	14 (12.2%)	5 (21.7%)	6 (16.2%)	1 (4.0%)	2 (6.7%)		
Non LBBB IV delay	11 (9.6%)	3 (13.0%)	3 (8.1%)	2 (8.0%)	3 (10.0%)		
LBBB according to guidelines						0.516	
QRS > 150 ms	64 (55.7%)	11 (47.8%)	18 (48.6%)	16 (64.0%)	19 (63.3%)		
QRS 130-150 ms	29 (25.2%)	4 (17.4%)	13 (35.1%)	6 (24.0%)	6 (20.0%)		
MRI measurements							
End-diastolic volume (mL)	241.6 ± 83.9	203.6 ± 78.9	229.2 ± 75.8	244.3 ± 75.2	284.1 ± 89.3	**0.003**	
End-systolic volume (mL)	149.5 (108.0)	112.0 (118.0)	142.0 (73.0)	157.0 (109.0)	190.0 (127.0)	**0.002**	0.000
LVEF (%)	34.0 ± 11.6	40.7 ± 11.3	35.3 ± 11.5	32.6 ± 8.6	28.1 ± 11.6	**< 0.001**	
LGE*						0.846	
None	46 (40%)	8 (34.8%)	17 (45.9%)	11 (44%)	10 (33.3%)		
Ischemic	32 (27.8%)	7 (30.4%)	11 (29.7%)	8 (32%)	6 (20.0%)		
Non-ischemic	31 (27%)	7 (30.4%)	7 (18.9%)	6 (24%)	11 (36.7%)		
Dyssynchrony measurements							
Septal flash						**< 0.001**	
Mild	36 (31.3%)	17 (73.9%)	15 (40.5%)	2 (8%)	2 (6.7%)		
Moderate	40 (34.8%)	5 (21.7%)	17 (45.9%)	10 (40%)	8 (26.7%)		
Prominent	39 (33.9%)	1 (4.3%)	5 (13.5%)	13 (52%)	20 (66.7%)		
Lateral to septal peak delay (ms)—A3C	223.1 ± 118.8	168.8 ± 137.8	259.1 ± 116.7	243.1 ± 115.9	205.7 ± 90.9	0.029	
Posterior to septal peak delay (ms)—A4C	222.1 ± 105.3	202.5 ± 126.2	241.0 ± 117.2	218.9 ± 73.9	217.5 ± 96.5	0.602	
Anterior IVS to posterior peak delay (ms)—PSAX	186.3 ± 101.8	150.3 ± 110.9	191.8 ± 122.9	197.4 ± 70.7	198.4 ± 86.1	0.297	
GLS	−8.1 ± 3.6-	−10.3 ± 3.31	−8.4 ± 3.7	−7.3 ± 3.0	−6.8 ± 3.3	**0.001**	
GLS 3D	−5.9 (4.1)	−7.1 (2.8)	−5.9 (5.0)	−5.0 (3.5)	−4.4 (5.2)	0.092	0.019
GRS	12.3 (9.8)	18.1 (13.1)	13.6 (9.7)	11.2 (8.7)	10.8 (8.8)	**0.002**	0.000
GRS 3D	13.2 (11.9)	20.1 (17.9)	13.7 (11.3)	11.2 (8.9)	9.9 (9.4)	0.009	0.001
GCS	−9.8 ± 3.9	−12.1 ± 4.1	−10.2 ± 6.1	−9.4 ± 3.1	−7.8 ± 3.8	**< 0.001**	
GCS 3D	−10.4 ± 4.4	−12.9 ± 4.5	−11.2 ± 3.9	−9.9 ± 5.3	−8.0 ± 4.4	< 0.001	

BMI body mass index, *LBBB* left bundle branch block, *A3C/A4C* apical 3/4 chambers, *PSAX* parasternal short axis, *GLS/GRS/GCS* global longitudinal/ radial/ circumferential strain

**n = 109, 6 missings*

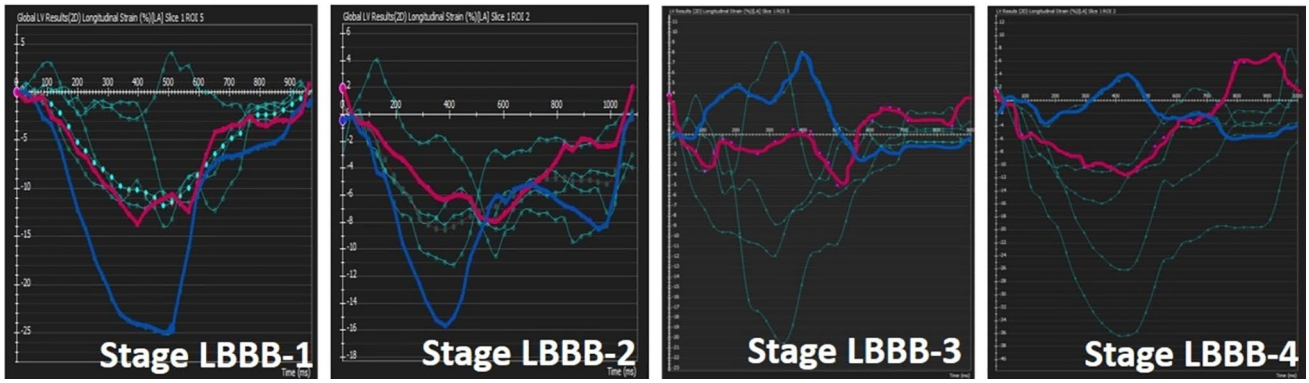

Fig. 4 Stages of LBBB-induced LV remodeling according to longitudinal strain curves. Different lines represent the strain curves of different myocardial segments of LV. From left to right, patterns 1 to 4 are represented, with anteroseptal wall colored red and the inferolateral wall blue.

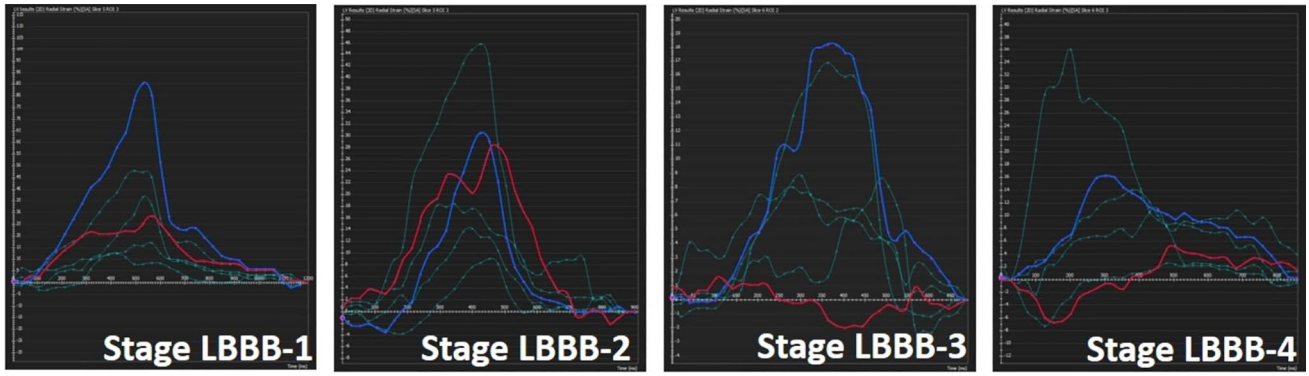

Fig. 5 Stages of LBBB-induced LV remodeling according to radial strain curves. Different lines represent the strain curves of different myocardial segments of LV. From left to right, patterns 1 to 4 are represented, with anteroseptal wall colored red and the inferolateral wall blue

the strain-based stages. According to literature the correlation between strain values in CMR and echocardiography is variable [29, 30]. One study showed good agreements between myocardial tagging and two-dimensional STE for GLS and GCS [31]. Another study showed modest correlation between CMR-FT and STE global strain values, with GLS being systematically lower in CMR, whereas global radial strain and GCS were higher in CMR than in STE [9].

It is noteworthy that these two techniques are based on different principles of image acquisition and reconstruction which may interfere in reproducibility between modalities. While STE relies in real-time images, FT-CMR relies on data acquired from different cardiac cycles [32]. Although, the temporal resolution is higher in echocardiography compared with CMR, CMR provides a superior signal-to-noise ratio and echocardiography may be limited by suboptimal acoustic windows and thus suboptimal endocardial delineation. All these differences may be considered a limitation for comparison both methods and may also impact the feature tracking analysis. However previous studies have shown a good intramodal agreement for GLS between the two modalities and also a superior reproducibility compared with ejection fraction measurement [33].

Our study did not focus on the relationship between LBBB patterns and CRT response, however according to recent studies LBBB-1 pattern was associated with less favorable ventricular remodeling after CRT [4, 5, 15, 34, 35] and LBBB-4, the final stage of LBBB, had the most adverse remodeled LV [6]. The double peaked pattern LBBB-2 and LBBB-3 stages, in the middle, were considered a marker for CRT response [36], being the ones that will benefit most from this strategy. We might speculate that CMR-FT analysis could be of value in assessing the prognosis and choosing the therapeutic strategy, namely candidacy to CRT, in patients with LBBB. Additional information is needed to find prognostic value of strain patterns regarding CRT clinical response and major cardiovascular events. Additionally, there are no standardization for CMR strain values which might be crucial to introduce this methodology in future clinical practice.

Despite significant LV remodeling in later stages of LBBB strain patterns, neither QRS duration or

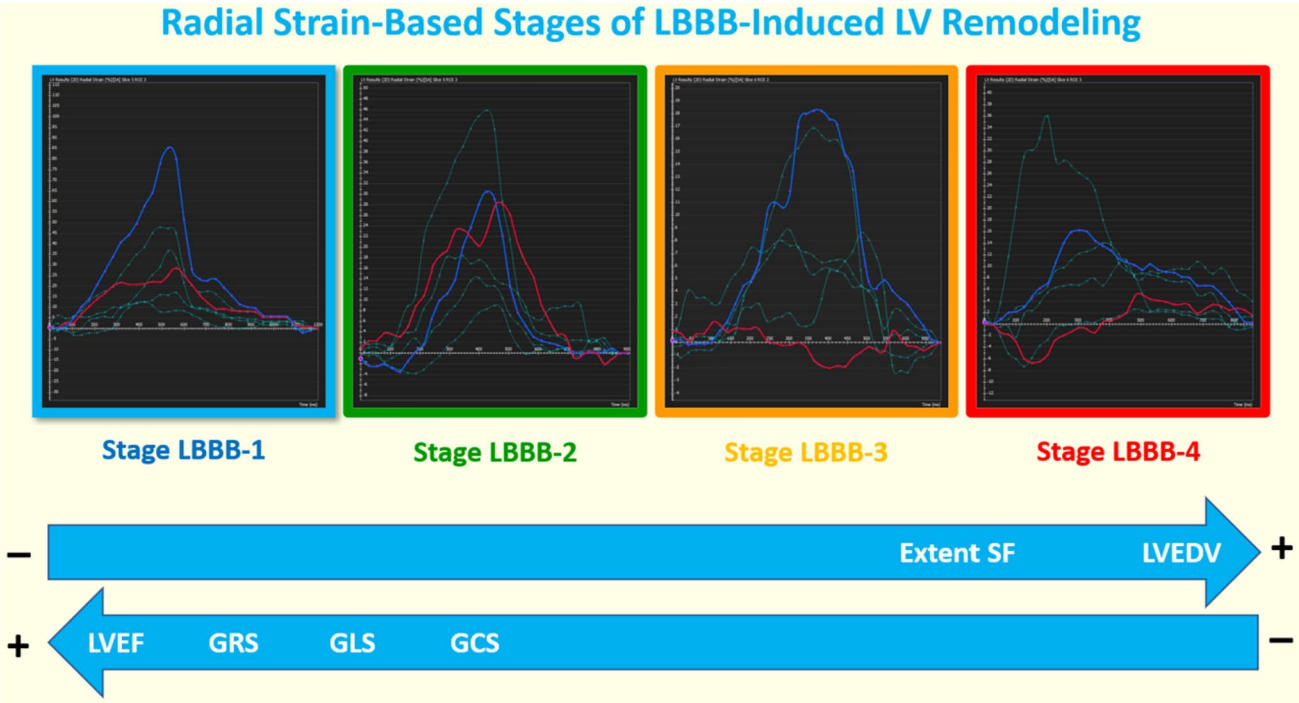

Fig. 6 Strain-based stages of LBBB-induced LV remodeling. The 4 stages of LBBB-induced radial strain patterns and their relationship with LV adverse remodeling and SF

septal-to-lateral wall delay were significant higher in those patients. Previous studies have confirmed our findings of weak or no correlation between QRS duration and myocardial deformation [12, 26, 37]. Baritussio et al. also found that there was no significant difference in QRS duration between ischemic, non-ischemic heart disease patients and patients with isolated LBBB-related septal dyssynchrony, despite differences regarding myocardial strain assessed by CMR [26].

Some studies propose that, in CRT candidates, STE should be complemented by CMR for accurate assessment of viability, especially for patients with ischemic etiology [25, 38]. It is believed that LV lead should be placed on the most delayed site, avoiding myocardial scar [39], in order to prevent inefficient stimulation in that territory [40]. With this in mind we hypothesized that the presence of myocardial scar (lateral, septal or both) would influence the strain pattern and the stage of LBBB and LV remodeling. In our population, LGE was found in 55% of the patients, half of them with ischemic pattern. Contrary to our expectations, we have found no differences in LGE across different patterns of myocardial strain (ischemic vs non-ischemic). This may be the result of small sample size, but may also reflect the complex relationship between myocardial fibrosis and intraventricular conduction delays. In the literature there is controverse data regarding the relationship between LGE and LBBB. While Grigoratos et al.suggest that the presence of LBBB is associated with a higher prevalence and extent of LGE [41], Becker et al.concluded that in dilated cardiomyopathy, ventricular conduction delay was not correlated to the presence nor the extent of septal midwall LGE [42].

Limitations

Some limitations of this study should be acknowledged. First, since many of the patients had their echocardiograms performed in other institutions, we were unable to assess the concordance between echocardiographic and CMR classification of LBBB strain patterns. Second, the applicability of our findings may be limited by the single-center retrospective nature of this study, using a single specific software for myocardial strain analysis. The relatively small sample size may have limited the statistical power to identify certain associations, particularly the relationship between LGE and strain patterns. For the same reason, subgroup analysis (e.g. ischemic versus non-ischemic patients) could not be performed.

Conclusions

In patients with LBBB, CMR feature tracking may be used to classify myocardial septal strain into four different patterns, which correlate with the degree of LV remodeling

and dysfunction. In our population, the presence of LGE was similar across the different strain patterns, suggesting that myocardial fibrosis is not a major determinant in their development.

Acknowledgements None.

Author contributions MRS—Conceived and design the analysis and wrote the paper. MRS, MSS, SLP—Collected the data. MRS, SLP—Performed the analysis. All authors contributed to manuscript editing. All authors read and approved the final manuscript.

Funding None.

Data availability The data that support the findings of this study are available from the corresponding author upon request.

Declarations

Competing interests The authors declare that they have no competing interests.

Consent for publication All authors have read and agreed to the content, approve, and consent to the publication of this manuscript.

References

1. Kumar V, Venkataraman R, Wael A et al (2013) Implications of left bundle branch block in patient treatment. Am J Cardiol 111(2):291–300
2. Auffret V, Martin RP, Daubert C et al (2018) Idiopathic/Iatrogenic left bundle branch block-induced reversible left ventricle dysfunction: JACC state-of-the-art review. J Am Coll Cardiol 72(24):3177–3188
3. Smiseth OA, Aalen JM (2019) Mechanism of harm from left bundle branch block. Trends Cardiovasc Med 29(6):335–342
4. Calle S, Delens C, Kamoen V et al (2020) Septal flash: at the heart of cardiac dyssynchrony. Trends Cardiovasc Med 30(2):115–122
5. Risum N, Tayal B, Hansen T et al (2015) Identification of typical left bundle branch block contraction by strain echocardiography is additive to electrocardiography in prediction of long-term outcome after cardiac resynchronization therapy. J Am Coll Cardiol 66(6):631–641
6. Calle S, Kamoen V, de Buyzere M et al (2021) A strain-based staging classification of left bundle branch block-induced cardiac remodeling. JACC: Cardiovascular Imaging 14(9):1691–1702
7. Scatteia A, Baritussio A, Bucciarelli-Ducci C (2017) Strain imaging using cardiac magnetic resonance. Heart Fail Rev 22(4):465–476
8. Revah G, Wu V, Huntjens PR et al (2016) Cardiovascular magnetic resonance features of mechanical dyssynchrony in patients with left bundle branch block. Int J Cardiovasc Imaging 32(9):1427–1438
9. Pryds K, Larsen AH, Hansem MS et al (2019) Myocardial strain assessed by feature tracking cardiac magnetic resonance in patients with a variety of cardiovascular diseases—A comparison with echocardiography. Sci Rep 9(1):11296
10. Sohal M, Amraoui S, Chen Z et al (2014) Combined identification of septal flash and absence of myocardial scar by cardiac magnetic resonance imaging improves prediction of response to cardiac resynchronization therapy. J Interv Card Electrophysiol 40(2):179–190
11. Strauss DG, Selvester RH, Wagner GS (2011) Defining left bundle branch block in the era of cardiac resynchronization therapy. Am J Cardiol 107(6):927–934
12. Andersson LG, Wu KC, Wieslander B et al (2013) Left ventricular mechanical dyssynchrony by cardiac magnetic resonance is greater in patients with strict vs nonstrict electrocardiogram criteria for left bundle-branch block. Am Heart J 165(6):956–963
13. Kramer CM, Barkhausen J, Bucciarelli-Ducci C et al (2020) Standardized cardiovascular magnetic resonance imaging (CMR) protocols: 2020 update. J Cardiovasc Magn Reson 22:17
14. Gjesdal O, Remme EW, Opdahl A et al (2011) Mechanisms of abnormal systolic motion of the interventricular septum during left bundle-branch block. Circulation: Cardiovascular Imaging 4:264–273
15. Leenders GE, Lumens J, Cramer MJ et al (2011) Septal deformation patterns delineate mechanical dyssynchrony and regional differences in contractility analysis of patient data using a computer model. Circ Heart Failure 5(1):87–96
16. Breithardt G, Breithardt OA (2012) Left bundle branch block, an old-new entity. J Cardiovasc Transl Res 5:107–116
17. Sanna GD, Merlo M, Moccia E et al (2020) Left bundle branch block-induced cardiomyopathy: a diagnostic proposal for a poorly explored pathological entity. Int J Cardiol 299:199–205
18. Parsai C, Bijnens B, Sutherland GR et al (2009) Toward understanding response to cardiac resynchronization therapy: left ventricular dyssynchrony is only one of multiple mechanisms. Eur Heart J 30(8):885–886
19. Owashi K, Taconné M, Courtial N et al (2022) Desynchronization strain patterns and contractility in left bundle branch block through computer model simulation. J Cardiovascular Development Dis 9(2):53
20. Wang CL, Wu CT, Yeh YH et al (2017) Left bundle-branch block contraction patterns identified from radial-strain analysis predicts outcomes following cardiac resynchronization therapy. Int J Cardiovasc Imaging 33(6):869–877
21. Mondillo S, Galderisi M, Mele D et al (2011) Speckle-tracking echocardiography a new technique for assessing myocardial function. J Ultrasound Med 30(1):71–83
22. Onishi T, Saha SK, Ludwig DR et al (2013) Feature tracking measurement of dyssynchrony from cardiovascular magnetic resonance cine acquisitions: comparison with echocardiographic speckle tracking. J Cardiovasc Magn Reson 15:95
23. Fixsen LS, de Lepper AG, Strik M et al (2019) Echocardiographic assessment of left bundle branch-related strain dyssynchrony: a comparison with tagged MRI. Ultrasound Med Biol 45(8):2063–2074
24. Saporito S, van Assen HC, Houthuizen P et al (2016) Assessment of left ventricular mechanical dyssynchrony in left bundle branch block canine model: comparison between cine and tagged MRI. J Magn Reson Imaging 44(4):956–963
25. Bakos Z, Ostenfeld E, Markstad H et al (2014) A comparison between radial strain evaluation by speckle-tracking echocardiography and cardiac magnetic resonance imaging, for assessment of suitable segments for left ventricular lead placement in cardiac resynchronization therapy. Europace 16(12):1779–1786
26. Baritussio A, Biglino G, Moharem-Elgamal S et al (2021) Are all left bundle branch blocks the same? Myocardial mechanical implications by cardiovascular magnetic resonance. Int J Cardiol 324:221–226
27. Land V, Germans T, van Dijk J et al (2001) The effect of left bundle branch block on left ventricular remodeling, dyssynchrony and deformation of the mitral valve apparatus: an observational cardiovascular magnetic resonance imaging study. Int J Cardiovasc Imaging 23(4):529–536
28. Voigt JU, Pedrizzetti G, Lysyansky P et al (2015) Definitions for a common standard for 2D speckle tracking echocardiography:

consensus document of the EACVI/ASE/Industry Task Force to standardize deformation imaging. Eur Heart J Cardiovasc Imaging 16(1):1–11
29. Onishi T, Saha SK, Delgado-Montero A et al (2015) Global longitudinal strain and global circumferential strain by speckle-tracking echocardiography and feature-tracking cardiac magnetic resonance imaging: comparison with left ventricular ejection fraction. J Am Soc Echocardiogr 28(5):587–596
30 Rajiah PS, Kalisz K, Broncano J et al (2022) Myocardial strain evaluation with cardiovascular MRI: Physics, Principles, and Clinical applications. RadioGraph 42(4):968–990
31. Amzulescu MS, Langet H, Saloux E et al (2017) Head-to-head comparison of global and regional two-dimensional speckle tracking strain versus cardiac magnetic resonance tagging in a multicenter validation study. Circ Cardiovasc Imaging. https://doi.org/10.1161/CIRCIMAGING.117.006530
32. Pedrizzetti G, Claus P, Kilner P et al (2016) Principles of cardiovascular magnetic resonance feature tracking and echocardiographic speckle tracking for informed clinical use. J Cardiovasc Magn Reson 18:51
33. Aurich M, Keller M, Greiner S et al (2016) Left ventricular mechanics assessed by two-dimensional echocardiography and cardiac magnetic resonance imaging: comparison of high-resolution speckle tracking and feature tracking. Eur Heart J Cardiovasc Imaging 17(12):1370–1378
34. Menet A, Bernard A, Tribouilloy C et al (2017) Clinical significance of septal deformation patterns in heart failure patients receiving cardiac resynchronization therapy. Eur Heart J Cardiovasc Imaging 18(12):1388–1397
35. Maréchaux S, Guiot A, Castel AL et al (2014) Relationship between two-dimensional speckle-tracking septal strain and response to cardiac resynchronization therapy in patients with left ventricular dysfunction and left bundle branch block: a prospective pilot study. J Am Soc Echocardiogr 27(5):501–511
36. Risum N, Jons C, Olsen NT et al (2012) Simple regional strain pattern analysis to predict response to cardiac resynchronization therapy: rationale, initial results, and advantages. Am Heart J 163(4):697–704
37. Bleeker GB, Schalij MJ, Molhoek SG et al (2004) Relationship between QRS duration and left ventricular dyssynchrony in patients with end-stage heart failure. J Cardiovasc Electrophysiol 15(5):544–549
38. White JA, Yee R, Yuan X et al (2006) Delayed enhancement magnetic resonance imaging predicts response to cardiac resynchronization therapy in patients with intraventricular dyssynchrony. J Am Coll Cardiol 48(10):1953–1960
39. Spragg DD, Dong J, Fetics BJ et al (2010) Optimal left ventricular endocardial pacing sites for cardiac resynchronization therapy in patients with ischemic cardiomyopathy. J Am Coll Cardiol 56(10):774–781
40. Khan FZ, Virdee MS, Palmer CR et al (2021) Targeted left ventricular lead placement to guide cardiac resynchronization therapy: The TARGET study: a randomized, controlled trial. J Am Coll Cardiol 59(17):1509–1518
41. Grigoratos C, Liga R, Bennati E et al (2018) Magnetic resonance imaging correlates of left bundle branch disease in patients with nonischemic cardiomyopathy. Am J Cardiol 121(3):370–376
42 Becker MAJ, Allaart CP, Zweerink A et al (2020) Correlation between septal midwall late gadolinium enhancement on CMR and conduction delay on ECG in patients with nonischemic dilated cardiomyopathy. IJC Heart and Vasculature. 26:100474
43 Delgado V, Ypenburg C, van Bommel RJ et al (2008) Assessment of left ventricular dyssynchrony by speckle tracking strain imaging. Comparison between longitudinal, circumferential, and radial strain in cardiac resynchronization therapy. J Am Coll Cardiol. 51(20):1944–1952
44. Obokata M, Nagata Y, Wu VC et al (2016) Direct comparison of cardiacmagnetic resonance feature tracking and 2D/3D echocardiography speckle tracking for evaluation of global left ventricular strain. Eur Heart J Cardiovasc Imaging 17(5):525–532
45 Erley J, Genovese D, Tapaskar N et al (2019) Echocardiography and cardiovascular magnetic resonance-based evaluation of myocardial strain and relationship with late gadolinium enhancement. J Cardiovascular Magn Resonance 21(1):46